Structural study of amorphous CoFeB thin films exhibiting in-plane uniaxial magnetic anisotropy

D. Kirk,[1] A. Kohn,[1,*] K. B. Borisenko,[1] C. Lang,[1] J. Schmalhorst,[2] G. Reiss,[2] and D. J. H. Cockayne[1]
[1]*Department of Materials, University of Oxford, Oxford OX1 3PH, United Kingdom*
[2]*Department of Physics, Thin Films and Physics of Nanostructures, Bielefeld University, 33501 Bielefeld, Germany*
(Received 23 July 2008; revised manuscript received 18 October 2008; published 9 January 2009)

The structure of amorphous ferromagnetic $Co_{40}Fe_{40}B_{20}$ thin films, in particular the origin of induced magnetic in-plane anisotropy, is investigated by reduced density function (RDF) analysis of electron-diffraction patterns. In this research, the RDF methodology is developed in order to measure the direction-dependent bond lengths and coordination numbers. The directional variations in these parameters are predicted to be the likely origins of induced anisotropy. With nearest-neighbor distances measured to an accuracy of 0.02 Å, no variations in the characteristic bond lengths with direction are observed. By studying the coordination numbers, it is shown that any directional ordering effect must be less than 5% and 1% for transition-metal–metalloid and transition metal-transition metal neighbors, respectively, in CoFeB films subjected to a 400 Oe magnetic field during deposition. The overall structure of $Co_{40}Fe_{40}B_{20}$ thin films is further investigated by reverse Monte Carlo simulations, which enable an estimation of the coordination number of the transition-metal components in the CoFeB alloy. These simulations find a range of local coordination polyhedra present in the material. Despite an average coordination number of approximately 8 for the transition-metal component, a degree of medium-range order, and a stoichiometry close to $Co_{50}Fe_{50}$, large local deviations from this octahedral value mean that the structure is not based on bcc-type basic units.

DOI: 10.1103/PhysRevB.79.014203 PACS number(s): 61.05.J−, 75.50.Kj, 75.30.Gw, 68.37.Lp

I. INTRODUCTION

Amorphous ferromagnetic materials based on combinations of transition-metal (TM) and metalloid (M) atoms (e.g., CoFeB) are of great technological importance, not least because of their use in tunnel magnetoresistance structures[1] and other novel devices.[2] Long-range structural order is not necessary for a material to exhibit ferromagnetic properties;[3] because of the nature of the exchange interaction, short-range order is far more significant. These materials can be fabricated to exhibit an in-plane uniaxial magnetic anisotropy in any arbitrary direction, for example, by annealing within a magnetic field.[4] This experimental observation is somewhat surprising given that the amorphous low structural order is retained as opposed to highly ordered materials in which the crystal fields result in magnetic anisotropy. In-plane magnetic anisotropy in soft magnetic films is a required property for the operation of devices such as magnetic tunnel junctions for sensor applications. Strong uniaxial magnetic anisotropy has also been observed in rare-earth–transition-metal (RE-TM) thin films[5–8]—most notably FeTb—though in these systems the magnetic easy axis tends to be out of plane.

There is clearly a structural origin of this anisotropy, which is short range due to exchange interactions. Two possible explanations have been offered: first, bond-orientation anisotropy (BOA) postulates that more near neighbors (i.e., a higher density of bonds) will be found in the plane of the film compared to perpendicular to it. This is supported by the work of Yan *et al.*[5] who performed x-ray scattering experiments on TbFeCo films. However, no quantitative analysis of the coordination number change is presented in their work.

In contrast to BOA, which does not predict anisotropy in the chemical ordering of near-neighbor atoms, pair-ordering anisotropy (POA) (an atomic scale rearrangement outlined in Néel's pair-ordering model[9]) postulates a difference in the number of like and unlike nearest-neighbor distances for the in-plane and out-of-plane directions as the cause of magnetic anisotropy. Harris *et al.*[6] used polarization-dependent extended x-ray-absorption fine structure (EXAFS) to show that FeTb films exhibit a preference for unlike (Tb-Fe) near neighbors to align preferentially in the out-of-plane direction. Further support of the pair-ordering model was provided by Hufnagel *et al.*[7] who, in their work on FeTb thin films, found a greater number of Tb-Fe bonds in the out-of-plane direction—in some cases the measured change was greater than 10%. They also observed an opposite effect to Yan *et al.*,[5] in that the overall coordination number was found to be greater in the out-of-plane direction. In addition they reported small changes in the bond lengths with evidence of a slight contraction in the plane (0.02, 0.03, and 0.05 Å for Fe-Fe, Fe-Tb, and Tb-Tb bonds, respectively) compared to perpendicular to it. They concluded that the type of coordination, and not merely the overall coordination number, determines the perpendicular magnetic anisotropy. More recently, Harris and Pokhil[8] showed that the preference for unlike atom pairs in the out-of-plane direction is promoted by selective resputtering of some configurations of Fe/Tb adatoms during the growth process.

In summary, the experimental evidence makes the pair-ordering model a more compelling explanation of the anisotropy in RE-TM materials than the BOA model. The source of this anisotropy is a relatively larger number of like atom pairs in the in-plane direction and unlike atom pairs perpendicular to the film.

Some attempts have been made to study the anisotropic short-range order of TM-M amorphous ribbons (e.g., using x-ray[10] and neutron diffraction[11]) but no experimental observations of variations in short-range order have been made of amorphous thin-film TM-M ferromagnets. This distinction is important because stress and compositional variations on a

macroscopic scale may play a role in magnetic anisotropy in ribbons with thicknesses in the micrometer scale (e.g., Ref. 12) whereas such effects are unlikely in thin (15 nm) films.

The family of TM-M alloys has been widely studied and observations consistent with the POA model have been made; these are that the strength of the induced anisotropy has been shown to be strongly dependent on composition, and also the overall anisotropy is known to be due to both TM-TM and TM-M interactions. Luborsky and Walker[13] showed that the strength of the anisotropy in a system with two transition metals reaches a maximum when the atomic ratio of the two metals is 1:1. The magnitude of K_u, the uniaxial anisotropy energy density, is typically around 10^3 J m^{-3} for amorphous TM-M alloys but much larger for RE-TM alloys. Harris and Pokhil[8] showed that K_u scales exponentially with the measured difference in in-plane and out-of-plane coordination number and that an FeTb alloy with a perpendicular magnetic anisotropy of 10^5 J m^{-3} is correlated with a 4% change in the Fe coordination number in plane and out of plane.

To our knowledge, no reports have calculated the change in coordination that is expected for the amorphous system examined in this work. O'Handley[14] estimated, based on Néel's pair-ordering theory,[9] that the coordination change due to ordering in an applied field in a crystalline interstitial system is less than 1%. This and the experimental evidence from RE-TM systems described above suggest that any coordination number change in the CoFeB thin films investigated here is likely to be approximately 1% or less.

This paper reports the use of electron diffraction to measure quantitatively the short-range order in thin CoFeB films in order to gain insight into the structural origins of magnetic-field-induced uniaxial anisotropy. Additionally, our aim is to obtain detailed structural information for this technologically important material. Such information can then be used in developing the theoretical explanation for large tunneling magnetoresistance ratios in magnetic tunnel junctions with amorphous ferromagnetic electrodes.[15] Using electron diffraction is advantageous for studying quantitatively such thin films (15 nm thick), which are comparable to those used in spin-electronic devices.

The experimental methods and theory of extracting pair-distribution functions from electron-diffraction patterns are summarized, with emphasis on the method for evaluating changes in the in-plane coordination number and near-neighbor distances. Reverse Monte Carlo (RMC) simulations are used to refine model structures against experimental pair-distribution functions.

II. EXPERIMENTAL METHODS

A. Sample preparation and magnetic properties

$Co_{40}Fe_{40}B_{20}$ films, 15 nm thick, were deposited by dc magnetron sputtering (with a deposition rate of approximately 0.2 nm s^{-1}) in an applied in-plane field of 400 Oe onto thin continuous carbon films (approximately 10–15 nm thick) supported by a copper grid. Carbon films were chosen in order to minimize the contribution of the substrate to the scattering of electrons and because they have very uniform thickness so that this additional scattering is constant for different areas of sample. The diffraction experiments were performed as soon as possible after deposition to minimize any possible oxidation of the samples. This approach was considered preferable to depositing a capping layer since this would also contribute to the diffracted intensity. As part of the deposition run, a $Co_{40}Fe_{40}B_{20}$ film was also deposited on an oxidized silicon wafer to allow bulk magnetic measurements to be made using an alternating-gradient magnetometer (Fig. 1). This shows that the expected hard- and easy-axis behaviors are observed in the $Co_{40}Fe_{40}B_{20}$ film in agreement with the direction of the applied magnetic field during deposition. K_u for this film was calculated as 1990 ± 170 J m^{-3}, determined by the energy difference along the hard and easy axes. As an aside, the sample was not subjected to any annealing treatment after deposition, which means, as Hirata *et al.*[16] showed, that the structure is expected to be homogenous and nanocrystalline regions are unlikely to form.

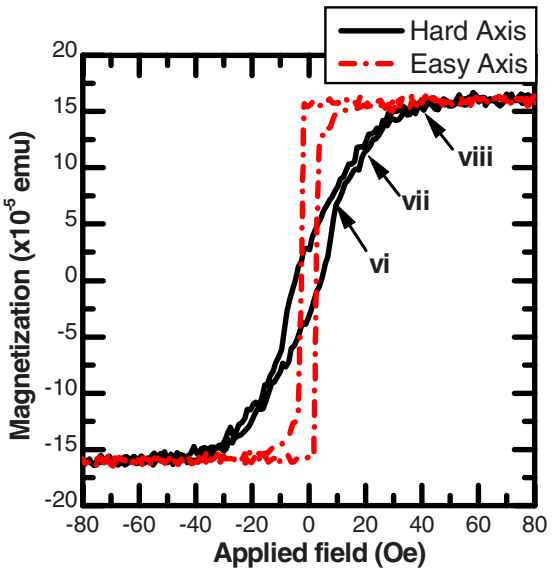

FIG. 1. (Color online) The magnetization curve for hard- and easy-axis reversals for CoFeB deposited on an oxidized silicon wafer. The numbered arrows correspond to the images from Fig. 2.

In order to verify that this behavior is replicated for the film deposited on the carbon-coated copper grids, Lorentz microscopy was used. The magnetization reversal of the $Co_{40}Fe_{40}B_{20}$ films was followed in real-time using the Fresnel mode of a JEOL 4000EX electron microscope operated at 400 kV, modified by using a low-field objective lens (AMG40) in which the specimen sits in a field-free (less than 1 Oe) region. A variable in-plane magnetic field between ± 400 Oe could be applied *in situ* using coils mounted in the sample holder. The magnetic field was applied along either the easy or hard axis. The direction of the easy axis was determined by observing the ripple contrast in underfocused Fresnel-contrast images and then aligning the sample relative to the applied magnetic field. This measurement was used to identify the easy- and hard-axis directions for the structural analysis.

Figure 2 shows images of the sample, with the magnetization of the sample being perpendicular to the ripple-type

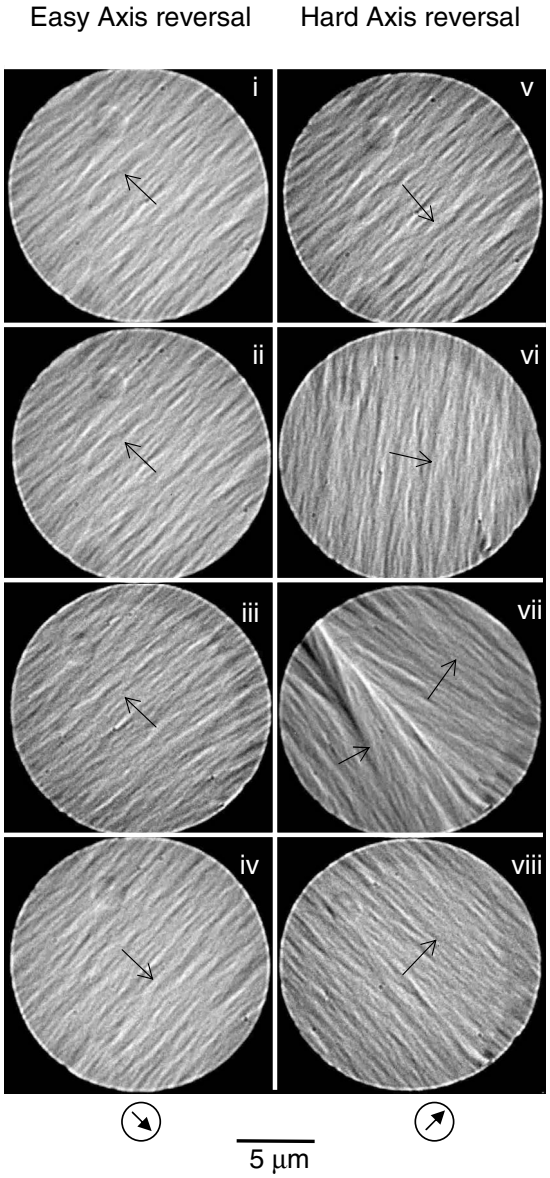

FIG. 2. Fresnel-contrast Lorentz TEM images showing magnetic reversal for [(i)–(iv)] field applied along the easy axis and [(v)–(viii)] field applied along the hard axis. The applied fields, the direction of which is shown by the encircled arrow, in Oe, are (i) 0, (ii) 2, (iii) 4, (iv) 6, (v) 0, (vi) 15, (vii) 25, and (viii) 40 and the direction of magnetization of the sample is shown by an arrow on the image.

contrast seen in the images. When a field is applied along the easy axis, magnetic reversal is seen to take place abruptly through domain-wall nucleation and propagation at a field of 6 Oe. In contrast, when the field is applied at 90° to the easy axis, the magnetization of the sample is seen to rotate gradually to the field direction, finally switching at 40 Oe. Both the easy- and hard-axes reversal fields measured in the Lorentz transmission electron microscope (TEM) are very similar to those of the CoFeB deposited on an oxidized silicon wafer as measured in the hysteresis curve presented in Fig. 1. This shows that, in this experiment, uniaxial in-plane anisotropy has been successfully introduced into the $Co_{40}Fe_{40}B_{20}$ films deposited onto the carbon membrane. Additionally, the direction of the easy-axis determined in the Lorentz TEM agrees with the alignment of the grid in the deposition chamber.

B. Structural measurements

Electron diffraction was used previously to study anisotropy in amorphous FeTb by Zweck and Trautsch.[17] Unlike most FeTb films where the magnetic easy-axis direction is out of plane and, as explained above, is a result of selective resputtering of various adatom configurations, Zweck and Trautsch[17] annealed the sample in a strong magnetic field to force the easy axis to lie in plane. Though no quantitative description of the directional ordering was given, the authors showed that the pair-distribution functions obtained from electron diffraction are significantly different for the hard- and easy-axis directions.

In this work electron-diffraction patterns were collected on a charge coupled device (CCD) (1024×1024 pixels) in a 300 kV JEOL 3000F FEGTEM, aligned for parallel illumination using an overfocused condenser lens and a small selected area aperture. The diameter of the area in the sample from which the electron diffraction was collected was approximately 100 nm. After alignment, the microscope settings were left constant during diffraction pattern collection; neither the objective lens nor the diffraction lens currents were changed since these can have the effect of rotating the projected diffraction pattern.

In conventional electron microscopes the sample sits very close to the objective lens, which produces a high magnetic field perpendicular to the plane of the sample (1–2 T). In order to verify that exposure to this magnetic field did not affect the magnetic properties of the sample it was analyzed using Lorentz microscopy before and after the diffraction experiment. The reversal mechanism of the sample magnetization, before and after exposure to the field of the objective lens during the diffraction experiments, was found to be identical with an easy-axis reversal at 6 Oe and a hard-axis reversal at approximately 40 Oe.

The diffraction pattern was calibrated with a silicon crystal sample and a diffraction pattern was obtained for calibration of future diffraction patterns. During the calibration of the diffraction pattern, variations in the directional response of the CCD were detected. By rotating the silicon sample and repeating the calibration the effective camera length was found to be dependent on the azimuthal angle in the diffraction pattern. Figure 3 plots the effective pixel size (in reciprocal space units) against the angle (relative to "north") on the CCD, together with a sine function obtained by a least-squares fit to the calibration data. Since the aim of this experiment is to study directional changes in the short-range order in different directions in the sample, this directional calibration of the diffraction pattern is critically important.

Following the calibration, diffraction patterns were taken from two regions of the CoFeB film with care taken that no unusual features were observed and that the area examined was not close to a copper grid bar. Immediately after this, the sample was removed from the microscope, the specimen rotated by 90° in the holder, and then reinserted. Diffraction patterns were then taken from two further regions. Similar

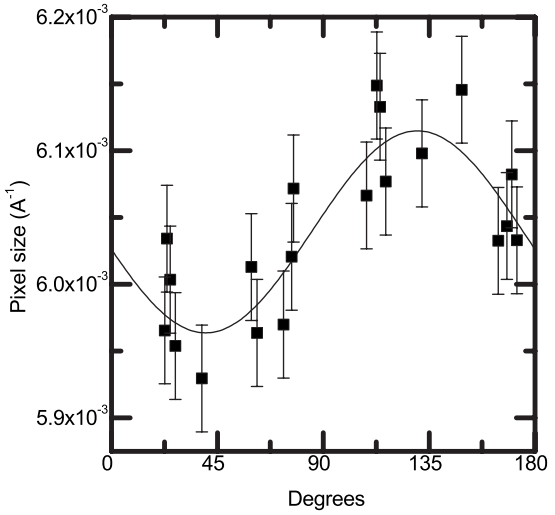

FIG. 3. The variation in effective pixel size with angle on the CCD. The line shows a sine function obtained by a least-squares fit to the data points.

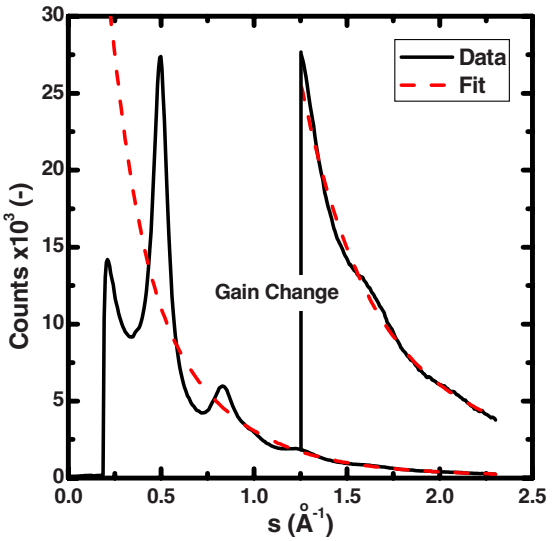

FIG. 4. (Color online) Intensity profile from an experimental diffraction pattern recorded from a thin film of CoFeB on a carbon substrate.

results were obtained from three different samples and here results from a single representative sample are presented. For each measurement, ten diffraction patterns were recorded and then summed for the reduced density function (RDF) analysis. This approach has the advantage of improving the signal-to-noise ratio and also verifying that no structural change occurred in the CoFeB thin film due to the exposure to the electron beam. The difference between individual diffraction patterns was negligible, thus enabling a direct summation.

The aim of this experiment is to search for structural differences between the hard- and easy-axis directions; therefore, it is vital to know the direction of the induced easy axis in diffraction space. The direction of the induced easy axis was marked on the copper grid and the angle between it and the grid lines was measured. During the collection of the diffraction patterns, an image of the grid was also taken hence allowing the direction of the easy axis to be known in an image. Since the grid edge is not completely straight and the images were taken at a relatively high magnification ($\times$200 000) some uncertainties in the angle of the grid bars, and hence the direction of the easy axis, is unavoidable; repeated measurements indicate that the grid angle can be measured to an accuracy of $\pm 4°$. Furthermore, there is a small rotation when switching between imaging and diffraction modes, which was measured as $6°$ ($\pm 1°$). As a consequence of the error from these two sources (the grid roughness and rotation between microscope modes) there is $\pm 5°$ uncertainty in the direction of the easy axis.

The center of the diffraction pattern was determined by choosing the position which minimized the difference in the profiles at $180°$ to each other. Trials showed that this gave a reproducibility of within approximately $\frac{1}{2}$ a pixel. After identifying the easy-axis direction in the diffraction pattern, radial profiles of the diffracted intensity were extracted from the diffraction patterns along the easy-axis direction and at intervals of $45°$. To increase the signal-to-noise ratio, seven profiles separated by $1°$ about each direction were averaged.

An example of the intensity profile plotted against scattering vector is shown in Fig. 4. The diffraction pattern data are collected out to approximately $s=3$ A^{-1}, where s is the scattering vector related to the scattering angle θ and electron wavelength λ by $s=2 \sin \theta/\lambda$. To remove the contribution to the diffracted intensity of the carbon support film, a diffraction pattern was obtained from a carbon-only area and this intensity was subtracted from the diffraction data before further analysis.

C. RDF methodology and data analysis

While the calculation of pair-distribution functions from electron-diffraction patterns is well established, the method is included here for clarity, especially concerning the method of calculating coordination numbers. Following Cockayne and McKenzie,[18] the scattered intensity $I(s)$ was converted to the reduced intensity function

$$\phi(s) = \frac{I(s) - N\langle f^2 \rangle}{N\langle f \rangle^2} s, \tag{1}$$

where

$$\langle f \rangle^2 = \left(\sum_i N_i f_i \right)^2 / N^2, \tag{2}$$

$$\langle f^2 \rangle = \left(\sum_i N_i f_i^2 \right) / N, \tag{3}$$

$$I(s) = Nf^2(s) + Nf^2(s) \int_0^\infty [g(r) - \rho_0] \frac{r}{s} \sin(sr) dr. \tag{4}$$

N is the number of atoms contributing to the diffraction pattern and N_i is the number of atoms of species i. f_i is the scattering factor of species i and ρ_0 is the average atomic density. The value of N was chosen to minimize the integral

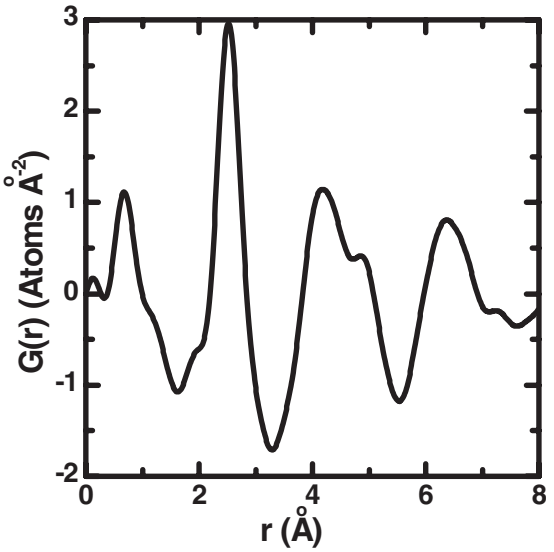

FIG. 5. $G(r)$ of CoFeB thin film. The peak positions correspond to characteristic bond lengths in the material.

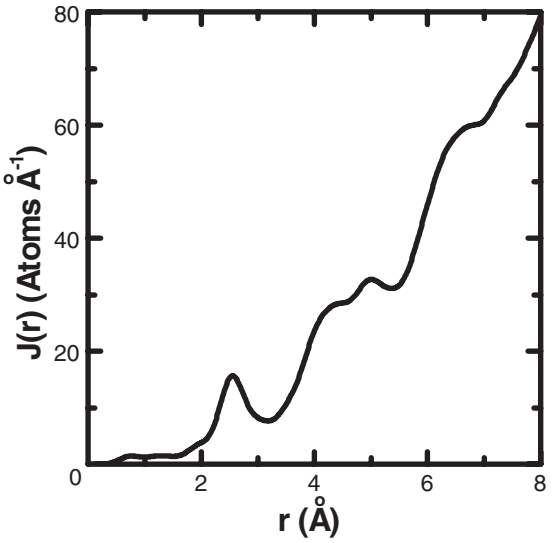

FIG. 6. $J(r)$ of CoFeB thin film. The TM-M contribution is visible at about 2 Å as a small shoulder on the strong TM-TM peak at 2.57 Å.

of $\Phi(s)$ between s_{max} and s_{min}. This is shown to give a good fit to the scattering data (see Fig. 4). Fourier transformation of the reduced intensity function gives $G(r)$, the reduced density function

$$G(r) = 8\pi \int_0^\infty \phi(s)\sin(2\pi sr)ds. \tag{5}$$

When the range of scattering vectors collected is finite, $G(r)$ can be expressed as

$$G(r) = 8\pi \sum_{s_{min}}^{s_{max}} \phi(s)\sin(2\pi sr)\exp(-bs^2), \tag{6}$$

where the damping parameter b is used to suppress high-frequency oscillations that appear due to the Fourier transform. A value of $b=0.3$ was chosen and was kept constant throughout. The Fourier transform is sampled every 0.01 Å. An example is shown in Fig. 5. In this method of evaluating the scattering data, the use of the sine transform implies isotropy in the specimen. Strictly, each $G(r)$ obtained from an intensity profile of the diffraction pattern is plotted as if referring to a sample that is isotropic in the plane. This prohibits a direct interpretation of the coordination number from a given directional profile but comparisons between $G(r)$ from different profiles are valid. For ease of calculating the coordination numbers, $J(r)$ can be plotted as shown in Fig. 6 (again strictly for isotropic samples) as

$$J(r) = rG(r) + 4\pi r^2 \rho_0, \tag{7}$$

where ρ_0 was measured as 8.0 ± 0.2 g cm^{-3} by x-ray reflectivity.

Prior to the investigation of the CoFeB thin films, the technique was tested on carbon thin film in which no anisotropy is expected. The $J(r)$ was calculated from intensity profiles in seven different directions of a diffraction pattern from the carbon film. The number of first nearest neighbors in the carbon film is given as

$$CN_{CC}(r_1, r_2) = \int_{1.00}^{1.98} J(r)dr = 3.31 \pm 0.09 \text{ atoms}, \tag{8}$$

where the error shown is two standard deviations from the average of all directions. The calculated value is very close to previous reports of the coordination of evaporated carbon films.[19] The error in the procedure is therefore shown to be relatively small in this case (two standard deviations is approximately 2.8%).

In the case of an alloy $G(r)$ is not simply the sum of the partial distribution functions, but a weighted sum.[20] If the peaks in the partial distribution functions are well separated, and if $f_i = K_i f(s)$ with K_i being a constant independent of s, then an average mutual coordination number can be defined as

$$CN_{ij}(r_1, r_2) = \frac{N\langle f\rangle^2}{(N_i + N_j)K_i K_j f^2} \int_{r_1}^{r_2} J(r)dr. \tag{9}$$

These may be reasonable approximations for some systems,[18] but they are not in the case of CoFeB since there is no satisfactory value of K that relates the scattering factors of Fe and B or Co and B. Consequently the approach used in this work is to study relative changes in the parameter

$$CN(r_1, r_2) = \int_{r_1}^{r_2} J(r)dr. \tag{10}$$

The minima in the $J(r)$ either side of the peak of interest were chosen arbitrarily as the limits of integration. The $CN_{TM\text{-}M}$ is defined as

$$CN_{TM\text{-}M}(r_1, r_2) = \int_{1.70}^{2.10} J(r)dr. \tag{11}$$

TABLE I. Bond lengths in CoFeB thin films.

Bond type	TM-M	First TM-TM	Second TM-TM	Third TM-TM	Fourth TM-TM
Bond length (Å)	2.00 ± 0.02	2.56 ± 0.02	4.27 ± 0.05	5.01 ± 0.04	6.38 ± 0.05

D. Reverse Monte Carlo simulations

Although absolute coordination numbers of an alloy cannot be calculated from the $J(r)$, RMC refinement of a starting atomic model against $G(r)$ can be used to produce a structural model consistent with the data, and from this coordination numbers for both the TM and M atoms can be deduced. The program used here is similar to that used by Keen and McGreevy.[21] An atomistic model of CoFeB was constructed as a cubic cell containing 200 atoms with a lattice parameter $a=12.695$ Å, corresponding to a density of 7.8 g cm^{-3} and periodic boundary conditions in three dimensions. The refinement was based on comparing the experimental reduced scattering intensity with that computed for the atomic model of the material. Contributions of the scattering intensity components that gave peaks below 1.5 Å in the experimental $G(r)$, where no contribution from the interatomic distances is expected, were removed using a Fourier filter. In the refinements an energy penalty term was also added based on the covalent radii of the elements to prevent unphysical solutions caused by close contacts between atoms. In all, four different refinements were performed in order to verify that the resulting model is independent of starting geometry. Three RMC refinements start from different randomly arranged positions of atoms. The last refinement uses bcc packing for Co and Fe with interstitial B atoms as the initial structure.

III. RESULTS

If the peaks in the partial pair-distribution functions are well separated then the peaks in $J(r)$ correspond to characteristic bond lengths in the material. In the case of CoFeB, the TM-TM partial pair-distribution function is of much greater magnitude than that of TM-M pairs and therefore the significant peaks correspond to TM-TM bond lengths. There is also a clear shoulder on the left-hand side of the first peak (see Fig. 6) which is attributed to the TM-M contribution to the $J(r)$.[22,23] By fitting two Gaussian functions (corresponding to the TM-TM and TM-M peaks) the TM-M peak position was determined.

All of the characteristic peak positions in $J(r)$ were then determined for directions along the eaxy axis, at 45° and at 90° to the easy axis. No correlations were found between the direction in the sample and the measured bond length. The average value for each peak position is given in Table I; the error shown is twice the standard deviation from the average of all measurements. In line with the pair-ordering model which explains the anisotropy in RE-TM alloys, we propose that magnetic anisotropy is likely to be caused by anisotropic bond distributions that give rise to changes in coordination number with direction in the sample.

To evaluate the TM-M coordination, rather than fitting a Gaussian curve, an integral was used since relative measurements are sufficient for detecting pair ordering and because better relative accuracy could be achieved. For each diffraction pattern, the integral is measured from each of the $J(r)$ obtained from radial profiles of the diffracted intensity. These integrals are then normalized to make the average integral for that diffraction pattern equal to unity. These values are shown in Fig. 7. The error bars are ± twice the standard deviation from the average value of the integral at each angular direction. The expected trend is plotted as a sine function as a guide to the eyes. It is based on the initial estimate of this work, derived from O'Handely,[14] that the coordination of unlike pairs is 1% greater perpendicular to the easy axis than along the easy axis. The values at intermediate angles are therefore expected to be equal and close to unity. However, these values are up to 5% from the average value, which gives an indication of the error involved in the calculation. Though these results do not demonstrate a trend, they do indicate an upper limit to the coordination change of 5%.

While it is likely that some chemical ordering between Fe and Co exists, electron diffraction is unable to distinguish between Fe-Fe, Fe-Co, and Co-Co contributions to the TM-TM peak. If the hypothesis of pair-ordering is appropriate for this system the coordination of unlike (Co-Fe) pairs will be different along and perpendicular to the easy axis. However, since Co and Fe are indistinguishable it is expected that the overall TM-TM coordination will be independent of direction. If on the other hand the BOA hypothesis is correct, one expects a change in the overall TM-TM coordination with direction. The TM-TM coordination parameter is the integral of $J(r)$ evaluated between the limits of 2.22 and

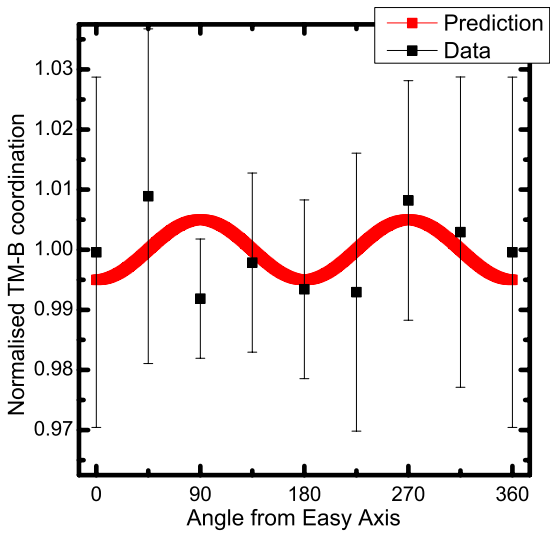

FIG. 7. (Color online) Normalized coordination numbers for TM-M bonding. The solid line is a guide for the eyes indicating the expected trend for a 1% change in TM-M coordination between hard- and easy-axis directions.

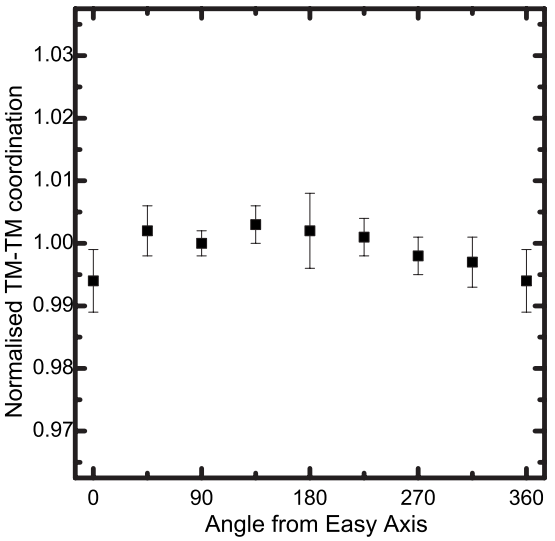

FIG. 8. Normalized coordination numbers for TM-TM bonding.

2.92 Å. The values of these integrals are shown in after the same normalization procedure described above. All of the calculated values lie within 1% of the average coordination with no observable trend. This result fits with both a pair-ordering-type change in coordination of undetermined size and also with the BOA hypothesis; though in this case an upper limit of about 1% can be given for the change in coordination of TM-TM pairs with direction (Fig 8).

To further study the structure of these thin films RMC modeling was used. Though the calculation of the total scattering intensity from a model uses Debye functions which assume no directional anisotropy in the structure, RMC modeling can still be used to investigate the structural units present and determine the overall coordination of the various elements. The correspondence of the experimental and model $G(r)$, seen in Fig. 9, is very good except for the region around 2.1 Å; this region is significant since it pertains to the TM-B bonding. After extensive testing we concluded that it most probably was due to contribution of extraneous scattering in this region such as the carbon support film. It was,

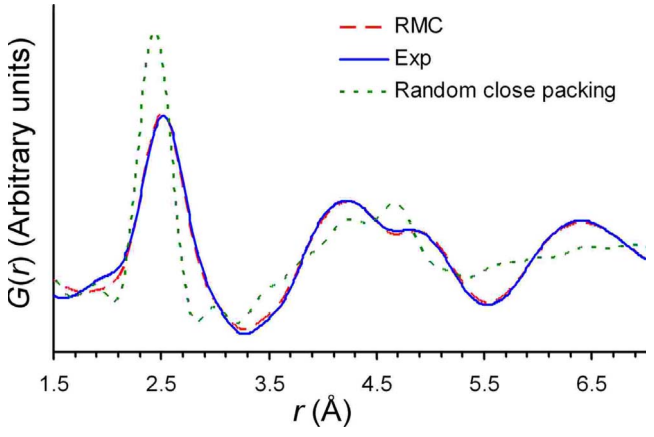

FIG. 9. (Color online) Comparison of experimental and model $G(r)$ and that obtained from a random close-packed structure.

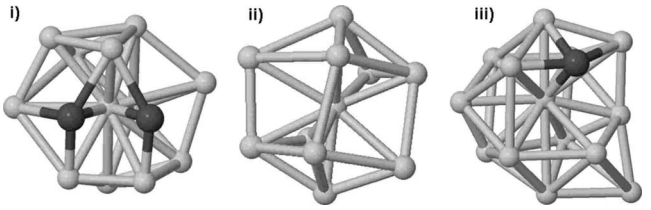

FIG. 10. Various structures observed in the refined model structure. TM atoms are light gray and B atoms are dark gray.

however, found that either subtracting this extraneous contribution from the experimental data or considering it in the analysis did not affect the average TM-B bond length determined from the refined models. The TM-B coordination number however was found to vary. All other structural parameters, in particular the TM-TM coordination number and average bond length, are believed to be accurately represented in the models. Figure 9 also shows a comparison of the experimental and model $G(r)$ along with $G(r)$ obtained from a model of a random close-packed structure. The significant differences of the experimental $G(r)$ from that of the random packing model, especially at larger interatomic distances, confirm the presence of medium-range order in the material. This ordering may be due to alignment of the coordination polyhedra relative to each other.

Following a fit to the experimental radial distribution function, the average TM-TM and TM-B distances were obtained as 2.5 ± 0.1 and 2.0 ± 0.1 Å, respectively. The large standard deviations here (compared to the values derived directly from the scattering data) were computed from the distances obtained in the same model and reflect the widths of distance distributions and distortions of the local structure. A small number of B-B bonds were also observed in the models with average length of 1.8 ± 0.1 Å. However, due to the small relative contribution to the total electron scattering by boron atoms, the RMC refinements alone cannot be relied upon either to confirm or to reject the formation of the B-B bonds in the studied material. Additionally, the structural parameters calculated from the RMC for the TM-B pairs should be treated with caution due to its small relative contribution to electron scattering when compared to the TM-TM pairs.

In the refined model of CoFeB distorted but regular coordination polyhedra could be discerned with different coordination numbers of the TM, as shown in Fig. 10. This variation leads to a high standard deviation of the average coordination numbers computed for the same model, 8 ± 3 for TM and 6 ± 2 for B. The average coordination numbers of TM and B are 8.6 ± 0.2 and 6.1 ± 0.2, respectively, when computed using several refined models starting from different initial arrangements. The coordination numbers computed in this way have small standard deviation reflecting the fact that all of the different starting models resulted in similar refined structures. The partial TM-TM, TM-B, B-TM, and B-B coordination numbers are 7.2 ± 0.2, 1.4 ± 0.1, 5.5 ± 0.2, and 0.6 ± 0.1, respectively. Since the average TM coordination number is 8.6, it may appear that the basic polyhedral unit of the metal atoms is close to a bcc octahedron. However, for each initial structural model, including the RMC

refinement starting from purely octahedral coordination, the refined structures are very similar, showing a large variety of structural units (e.g., Fig. 10). Importantly, the TM coordination was found to have substantial local variations, meaning that the structure cannot be described as a derivative of or a small distortion from a bcc crystal. Hirata *et al.*[16] reported a similar conclusion for as-quenched amorphous $Fe_{84}Nb_7B_9$ ribbons.

IV. CONCLUSIONS

This paper has described quantitatively the short- to medium-range order in amorphous CoFeB thin films, in which magnetic uniaxial anisotropy was induced during deposition. In order to detect the structural origin of this anisotropy, an electron-diffraction-based technique was developed. This technique was used to measure characteristic bond distances and relative coordination numbers in the plane of the film at various directions with respect to the magnetic easy axis. Nearest-neighbor bond lengths for TM-TM and TM-B bonds were found to be equal in all directions within the experimental accuracy of 0.02 Å.

The normalized coordination number of the TM-B and TM-TM bonds was constant with direction within the sensitivity of the technique, namely, 5% and 1%, respectively. We suggest that the cause of anisotropy is likely to be pair ordering and that its magnitude is less than 5% in the TM-B bonds. This conclusion is in agreement with the estimate of O'Handley.[14] However, we stress that it is important to expand the theoretical model to amorphous TM-B alloys in order to improve the accuracy of this estimate. The inability of the technique to distinguish between Co-Co, Co-Fe, and Fe-Fe bonding means that chemical ordering in the TM-TM bonding cannot be detected. If, as the BOA model predicts, there is a change in the overall TM-TM bonding with direction, it is not more than 1%.

RMC modeling was used to obtain actual coordination numbers for the TM and M atoms. It is necessary to be cautious in quantifying the results obtained by this method because of the methodology needed to extract the TM-B length and coordination number from the RDF. Nevertheless, the coordination number of the TM elements was found to be approximately 8.6, apparently similar to that of the bcc-type structure that would be expected in $Co_{50}Fe_{50}$. Furthermore, according to these RMC refinements, and recognizing the need for caution, it is evident that the addition of 20 at. % of the boron metalloid results in a large range of local coordination number of the metal atoms, namely, the structure cannot be described as a small distortion from a bcc crystal. Even though the addition of the metalloid element results in the loss of long-range order, a degree of medium-range order appears to be maintained when compared with random packing.

ACKNOWLEDGMENTS

A.K. acknowledges the financial support of the Royal Academy of Engineering and the EPSRC-GB.

*Corresponding author; amit.kohn@materials.ox.ac.uk

[1] D. D. Djayaprawira, K. Tsunekawa, M. Nagai, H. Maehara, S. Yamagata, N. Watanabe, S. Yuasa, Y. Suzuki, and K. Ando, Appl. Phys. Lett. **86**, 092502 (2005).
[2] T. Uhrmann, T. Dimopoulos, H. Brückl, V. K. Lazarov, A. Kohn, U. Paschen, S. Weyers, L. Bär, and M. Rührig, J. Appl. Phys. **103**, 063709 (2008).
[3] A. I. Gubanov, Sov. Phys. Solid State **2**, 468 (1960).
[4] B. Berry and W. C. Pritchett, Phys. Rev. Lett. **34**, 1022 (1975).
[5] X. Yan, M. Hirscher, T. Egami, and E. E. Marinero, Phys. Rev. B **43**, 9300 (1991).
[6] V. G. Harris, K. D. Aylesworth, B. N. Das, W. T. Elam, and N. C. Koon, Phys. Rev. Lett. **69**, 1939 (1992).
[7] T. C. Hufnagel, S. Brennan, P. Zschack, and B. M. Clemens, Phys. Rev. B **53**, 120204 (2006).
[8] V. G. Harris and T. Pokhil, Phys. Rev. Lett. **87**, 067207 (2001).
[9] L. Néel, J. Phys. Radium **12**, 339 (1951); **13**, 249 (1952).
[10] Y. Suzuki, J. Haimovich, and T. Egami, Phys. Rev. B **35**, 2162 (1987).
[11] D. Spilsbury, P. Butvin, N. Cowlam, W. S. Howells, and R. J. Cooper, Mater. Sci. Eng., A **226-228**, 187 (1997).
[12] S. C. Byeon, C. K. Kim, K. S. Hong, and R. C. O'Handley, Mater. Sci. Eng., B **60**, 58 (1999).
[13] F. E. Luborsky and J. L. Walker, IEEE Trans. Magn. **13**, 953 (1977).
[14] R. C. O'Handley, *Modern Magnetic Materials* (Wiley, New York, 2000), p. 521.
[15] M. Gradhand, C. Heiliger, P. Zahn, and I. Mertig, Phys. Rev. B **77**, 134403 (2008).
[16] A. Hirata, Y. Hirotsu, E. Matsubara, T. Ohkubo, and K. Hono, Phys. Rev. B **74**, 184204 (2006).
[17] J. Zweck and R. Trautsch, Cryst. Res. Technol. **35**, 689 (2000).
[18] D. J. H. Cockayne and D. R. McKenzie, Acta Crystallogr., Sect. A: Found. Crystallogr. **44**, 870 (1988).
[19] F. Li and J. S. Lannin, Phys. Rev. Lett. **65**, 1905 (1990).
[20] D. J. H. Cockayne, Annu. Rev. Mater. Res. **37**, 159 (2007).
[21] D. A. Keen and R. L. McGreevy, Nature (London) **344**, 423 (1990).
[22] N. Cowlam, J. Non-Cryst. Solids **205-207**, 567 (1996).
[23] T. Ohkubo and Y. Hirotsu, Phys. Rev. B **67**, 094201 (2003).